OPEN

Light: Science & Applications (2015) 4, e247; doi:10.1038/lsa.2015.20

www.nature.com/lsa

ORIGINAL ARTICLE

Get it white: color-tunable AC/DC OLEDs

Markus Fröbel[1], Tobias Schwab[1], Mona Kliem[1], Simone Hofmann[1], Karl Leo[1] and Malte C Gather[1,2]

Organic light-emitting diodes (OLEDs) have gained considerable attention because of their use of inherently flexible materials and their compatibility with facile roll-to-roll and printing processes. In addition to high efficiency, flexibility and transparency, reliable color tunability of solid state light sources is a desirable feature in the lighting and display industry. Here, we demonstrate a device concept for highly efficient organic light-emitting devices whose emission color can be easily adjusted from deep-blue through cold-white and warm-white to saturated yellow. Our approach exploits the different polarities of the positive and negative half-cycles of an alternating current (AC) driving signal to independently address a fluorescent blue emission unit and a phosphorescent yellow emission unit which are vertically stacked on top of each other. The electrode design is optimized for simple fabrication and driving and allows for two-terminal operation by a single source. The presented concept for color-tunable OLEDs is compatible with application requirements and versatile in terms of emitter combinations.
Light: Science & Applications (2015) **4,** e247; doi:10.1038/lsa.2015.20; published online 13 February 2015

Keywords: alternating current; color mixing; color tuning; vertical stacking; white organic light-emitting devices

INTRODUCTION

In recent years, organic light-emitting diodes (OLEDs) have evolved into a mature technology and OLEDs are now used in various display applications. OLEDs provide an internal charge-to-photon conversion efficiency of nearly 100% and deliver homogeneous emission over large areas, making them promising candidates for new and innovative lighting applications.[1] White OLEDs, in particular, offer great potential for energy-efficient general illumination: luminous efficacies of more than 90 lm W^{-1}, comparable to the best fluorescent tubes, have already been reported.[2,3] Furthermore, OLED-based light sources can be made mechanically flexible and transparent, offering new opportunities for architecture, visual art and decoration.[4] The reliable real-time tunability of the OLED emission color would impart further momentum to OLED technology on its way to becoming a widespread source of general illumination. Thus far, two different color-tuning concepts have prevailed in the literature. One exploits voltage-dependent changes in emission color and was demonstrated as early as 1994 for OLEDs fabricated from polymer blends.[5] Voltage-dependent color shifts are the result of a variety of mechanisms, e.g., voltage-dependent charge trapping, a spatial shift of the recombination zone, a modified exciton distribution, or exciton quenching at high current densities.[5–7] However, this approach has several drawbacks: not only are the mechanisms that lead to voltage-dependent color-shifts difficult to control, but adjusting the driving voltage also unavoidably results in a dramatic and undesired change in device brightness. The second concept overcomes the disadvantages of the voltage-controlled approach by using a stacked tandem OLED structure with two (or more) independently addressable units emitting light of different colors.[8,9] In comparison with the first method, this approach provides much greater control over the emission spectrum. However, to individually address each unit, an additional electrode must be added into the device stack as a connection between two adjacent units. This intermediate electrode must be transparent and therefore must be made either of a thin metal layer (~15 nm) or from indium tin oxide.[10] However, the deposition of indium tin oxide can be problematic due to sputter-induced damage to the organic material underneath,[11] whereas metal films absorb a significant amount of light and introduce additional micro-cavity effects.[12–14] Hence, the device development of highly efficient color-tunable OLEDs remains experimentally challenging: the color-tunable OLEDs that have been reported thus far demonstrate relatively modest efficiencies (<10% external quantum efficiency (*EQE*), <10 lm W^{-1}), despite the use of phosphorescent emitter systems.[15,16] Although these reports on vertical stacking of two independently controllable emission units have demonstrated only moderate performance, we believe that an efficient realization of such a system is a necessary and important step toward RGB full-color devices in which three independent emission units are stacked on top of each other. Such a vertically stacked RGB configuration is highly attractive for display applications as it allows for greatly increased pixel densities and a close-to-optimal utilization of the available display panel area for all colors.

In this work, we demonstrate highly efficient color-tunable white OLEDs based on a combination of a fluorescent blue emitting unit and a phosphorescent yellow emitting unit for the generation of white light. In contrast to the majority of publications on this topic, our devices are driven by an alternating current (AC) signal, which allows us to reduce the required number of independently addressable electrodes from three to only two.[8,16–18] By using an ultrathin and highly

[1]Institute for Applied Photophysics (IAPP), Dresden University of Technology, D-01069 Dresden, Germany and [2]School of Physics and Astronomy, University of St Andrews, St Andrews KY16 9SS, UK
Correspondence: M Fröbel, Institute for Applied Photophysics (IAPP), Dresden University of Technology, George-Bähr-Str. 1, 01069 Dresden, Germany
E-mail: markus.froebel@iapp.de
Received 10 September 2014; revised 2 December 2014; accepted 2 December 2014; accepted article preview online 4 December 2014

transparent layer of highly conductive metal as the intermediate electrode,[19–21] our devices achieve efficiencies comparable to those of state-of-the-art non-color-tunable white OLEDs with the additional advantage of providing continuous color tuning at constant brightness from deep blue through cold-white and warm-white to saturated yellow. Our device efficiencies of up to 36.8 lm W^{-1} at warm-white color coordinates are—to the best of our knowledge—the highest values achieved thus far for any freely color-tunable white OLED. Furthermore, we compare the performance of three different emitters within the blue emitting unit and provide general design rules to achieve high luminous efficacies (*LEs*) in such devices. We refer to our devices as AC-driven direct-current (DC) OLEDs, or AC/DC OLEDs, to clearly distinguish them from capacitively coupled OLEDs, which operate without direct charge injection from the electrodes and which are frequently referred to as 'AC-OLEDs'.[22–24]

MATERIALS AND METHODS

Our device architecture comprises a yellow phosphorescent pin-OLED stacked on top of a blue fluorescent pin-OLED, as schematically illustrated in Figure 1a.[25] Internally, our devices contain three electrodes (labeled E1, E2 and E3 in Figure 1a); however, E1 and E3 are electrically connected inside the device and thus, are at the same potential upon application of a voltage and can be addressed *via* a single external contact. E2 is the independent counter-electrode. The polarity between E1/E3 and E2 controls whether the blue- or the yellow-emitting sub-unit of the device is active: when E1/E3 is placed at a positive potential with respect to E2, we observe blue emission because the blue sub-unit is biased in forward direction, whereas the yellow sub-unit is biased in reverse direction and thus exhibits a negligible current density and no yellow emission. Upon a change in polarity, i.e., the application of a negative voltage to E1/E3, the device emits yellow light, as it is now the yellow-emitting sub-unit that is biased in forward direction. This polarity-dependent emission is depicted in Figure 1b. To study the influence of the blue-emitting sub-unit on the performance and color tunability of our AC/DC OLEDs, we investigated three different blue sub-units based on the blue fluorescent emitters 4P-NPD (sample S1), PPIP (sample S2) and MADN:TBPe (sample S3) (Figure 1c).

All layers were deposited in a UHV chamber at a base pressure of approximately 10^{-8} mbar onto glass substrates coated with structured tin-doped indium oxide, which served as a transparent bottom electrode. The thickness and deposition rates of the organic materials were measured *via* quartz crystal monitoring. The evaporation rates varied from 0.3 Å s^{-1} for the emission layer to 1 Å s^{-1} for the p- and n-type layers. Doping was realized by co-evaporation of the matrix material and the dopant.

As the p-type layers, we used 2,2′,7,7′-tetrakis-(N,N-di-methylphenylamino)-9,9′-spirobifluorene (Spiro-TTB) doped with 4 wt-% 2,2′-(perfluoronaphthalene-2,6-diylidene)dimalononitrile (F6-TCNNQ). The n-type layers consist of 4,7-diphenyl-1,10-phenanthroline (BPhen) doped with cesium (Cs). For the blue emission layer, either N,N'-di-1-naphthalenyl-N,N'-diphenyl-[1,1′:4′,1′′:4′′,1′′′-quaterphenyl]-4,4′′′-diamine (4P-NPD), 4,4′-bis(1-phenyl-1H-phenanthro[9,10-d]phenanthroimidazol-2-yl)biphenyl (PPIP) or 2-methyl-9,10-bis(naphthalen-2-yl)anthracene (MADN) doped with 1.5 wt-% 2,5,8,11-tetra-tert-butylperylene (TPBe) was used.[26] The yellow emission layer is a double-emission structure, fabricated from a combination of the primarily hole-conducting 4,4′,4′′-tris(N-carbazolyl)-triphenylamine (TCTA) matrix and the electron-conducting 2,2′,2′′-(1,3,5-phenylen)tris(1-phenyl-1H-benzimidazol) (TPBi) matrix, both doped with 8 wt-%

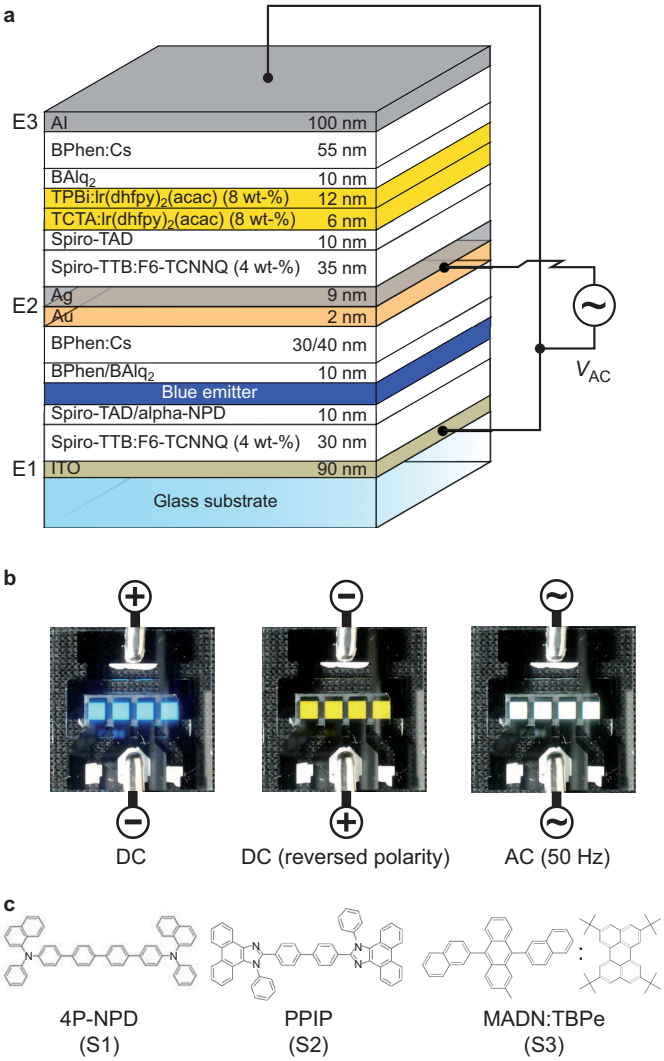

Figure 1 (**a**) Schematic illustration of the architecture of the investigated color-tunable AC/DC OLEDs with electrodes and wiring connected to an AC power supply (V_{AC}). Electrodes E1 and E3 are connected to each other and E2 is the independent counter electrode, allowing for two-terminal device operation using only one power supply. (**b**) Photographs showing an AC/DC OLED sample upon application of a DC bias (blue emission), a DC bias with reversed polarity (yellow emission), and an AC voltage with a frequency of 50 Hz (white emission). (**c**) Chemical structures of 4P-NPD, PPIP and MADN : TBPe which were the three blue emitter systems investigated in this study. AC, alternating current; DC, direct-current; OLED, organic light-emitting diode.

of the phosphorescent yellow emitter bis(2-(9,9-dihexylfluorenyl)-1-pyridine)(acetylacetonate)iridium(III) ($Ir(dhfpy)_2(acac)$). Electron- and hole-blocking layers (EBL/HBL) confine the charge carriers and excitons to the emission layer. In the case of the yellow-emitting unit, aluminum(III) bis(2-methyl-8-quninolinato)-4-phenylphenolate ($BAlq_2$) and 2,2′,7,7′-tetrakis-(N,N-diphenylamino)-9,9′-spirobifluorene (Spiro-TAD) were used as the HBL and EBL, respectively. The HBL/EBL combinations were different for the different blue-emitting units. In the case of 4P-NPD and PPIP, we used BPhen/Spiro-TAD and BPhen/N,N'-di(naphthalen-1-yl)-N,N'-diphenyl-benzidine (alpha-NPD), respectively. For MADN:TBPe, $BAlq_2$ was used as the HBL and alpha-NPD was used as the EBL. The highly transparent central multilayer electrode is a combination of 2 nm of gold (Au) and 9 nm of

doi:10.1038/lsa.2015.20

silver (Ag). An aluminum (Al) layer of 100 nm thickness was used as a highly reflective top electrode. E1 and E3 were processed using the same shadow mask. As the organic layers do not completely cover E1, the two electrodes have a direct electrical connection. In this way, our device design allows for easy fabrication and the internal connection between E1 and E3 requires no additional space on the substrate. The active area of the device is 6.49 mm^2. Prior to device investigation, the samples were encapsulated in a nitrogen glovebox.

The current–voltage–luminance (*j*–*V*–*L*) characteristics of our devices were measured using a source measure unit (SMU 2400; Keithley Instruments, Cleveland, Ohio, USA) in combination with a calibrated Si photo-diode. A calibrated spectrometer (CAS 140, Instrument Systems, Munich, Germany) recorded the spectral radiance in forward direction. Angle-dependent measurements were used to determine the *EQE* and *LE* of the blue and yellow units, respectively, and were performed in a spectrogoniometer setup that included a calibrated Ocean Optics USB4000 miniature spectrometer. The electrical characteristics of the device under AC driving were measured using a high-precision digital power meter (WT1600; Yokogawa, Tokyo, Japan). The WT1600 measures current, voltage and the phase angle between the two quantities to provide correct values for the dissipated power. The luminous flux under AC conditions was obtained in a calibrated integration sphere (LMS-100, d=250 mm; Labsphere, North Sutton, New Hampshire, USA).

RESULTS AND DISCUSSION

The electrode design of the AC/DC OLEDs allows independently investigating the electrical and optical characteristics of the yellow- and blue-emitting units under DC conditions by changing the polarity of the applied voltage. Figure 2 presents the *j*–*V*–*L* characteristics for each individual emission unit, as well as the *EQE* and *LE* of each unit. For a negative bias, only the yellow unit is active and the choice of the blue emitter should not influence the performance. Both the *j*–*V* characteristics and the *V*–*L* curves of the yellow unit are indeed identical for all three samples (Figure 2a). As expected, the differences in efficiency between the individual samples are also within the range of the sample-to-sample variation (Figure 2c). At a brightness of 1000 cd m^{-2}, we obtain *EQE*s of 15%–16% and *LE*s of 50–55 lm W^{-1} for the yellow units in the various samples. For the three different blue emitters, we observe very similar *j*–*V* behavior and only small differences in the *V*–*L* characteristics (Figure 2b). With regard to efficiency, the AC/DC OLED with 4P-NPD—a deep-blue emitter—exhibits the lowest *LE* of approximately 1.2 lm W^{-1} at 1000 cd m^{-2}, whereas the sky-blue emitter PPIP and the host:guest system MADN:TBPe yield *LE*s of 2.3 lm W^{-1} and 4.4 lm W^{-1}, respectively, as shown in Figure 2d. The *EQE* values of the three different blue units range from 2.5% in the case of PPIP and over 3.1% in the case of 4P-NPD to approximately 3.4% in the case of MADN:TBPe. The emission spectra of the blue- and the yellow-emitting units of samples S1, S2 and S3 are provided in Supplementary Fig. S1.

Upon application of an AC signal, the device alternately emits pulses of blue and yellow light. When a sufficiently high frequency is used, the human eye cannot resolve the separate emission from each unit, but instead perceives a color equivalent to the integrated emission over several operation cycles (cf. demonstration in Supplementary Movie 1 and Figure 1b). By modifying the pulse width and/or pulse height ratios between the positive and negative half-cycles of the AC signal, the relative contributions of blue and yellow emission can be adjusted, thereby allowing for tuning of the emission color perceived by the human eye (cf. demonstration in Supplementary Movie 2).

To study this color tuning in greater detail, we used a square-wave signal with equal pulse lengths in both the positive and negative half-cycles and tuned the emission color by varying the ratio between the voltages applied during the forward and backward pulses, as illustrated in the top row of Figure 3. The emission spectra for the three samples, S1, S2 and S3, are presented in the corresponding rows in Figure 3. For the spectra shown in columns 1 and 5, the voltage applied during either the negative or the positive half-cycle is zero, and pure emission from either the blue or the yellow unit can be observed. Column 3 represents the symmetric situation in which the absolute voltage applied during the forward and backward pulses is equal, leading to mixed emission from both units (cf. Figure 1b). Intermediate non-symmetric waveforms lead to a reduced contribution from one of the emission units (columns 2 and 4). Figure 4 presents the corresponding CIE coordinates for all emission spectra. The CIE coordinates associated with the different pulse forms are located along straight lines starting in the blue region and ending in the yellow region of the color space. The emission spectra of the pure yellow units are identical for S1, S2 and S3. As a result, all three samples are characterized by the same yellow color point in the CIE diagram while having different origins in the blue CIE region because of the different blue emitter systems used. As indicated by dotted lines in the CIE diagram in Figure 4, all color points on the connecting lines between the beginning and end points can be reached by changing the ratio of the

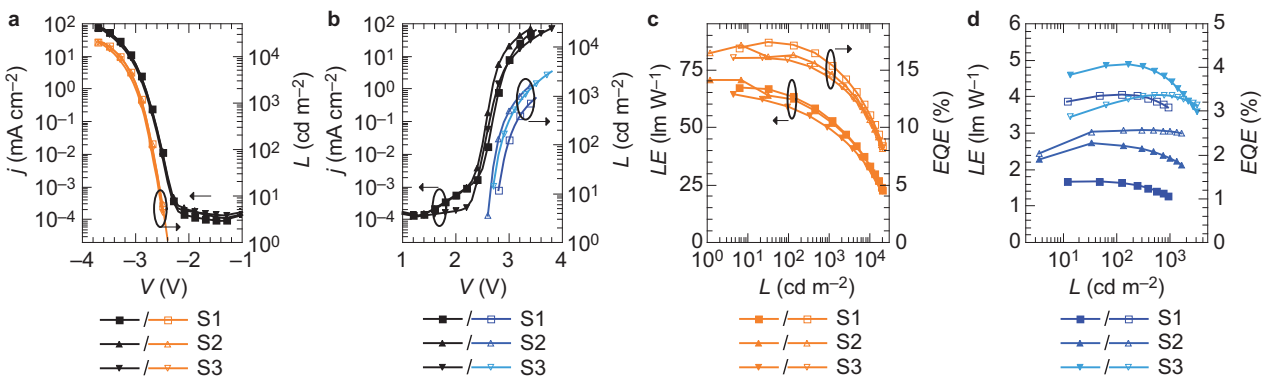

Figure 2 Current density (*j*) and luminance (*L*) as functions of voltage (*V*) for the (**a**) yellow-emitting units and (**b**) blue-emitting units of samples S1, S2 and S3. The corresponding *EQE* and *LE* values as functions of luminance are presented in (**c**) and (**d**) for the yellow and blue units, respectively. Data were acquired during DC operation, neglecting leakage currents through the reverse-biased opposite unit of the device. DC, direct-current; EQE, external quantum efficiency; LE, luminous efficacy.

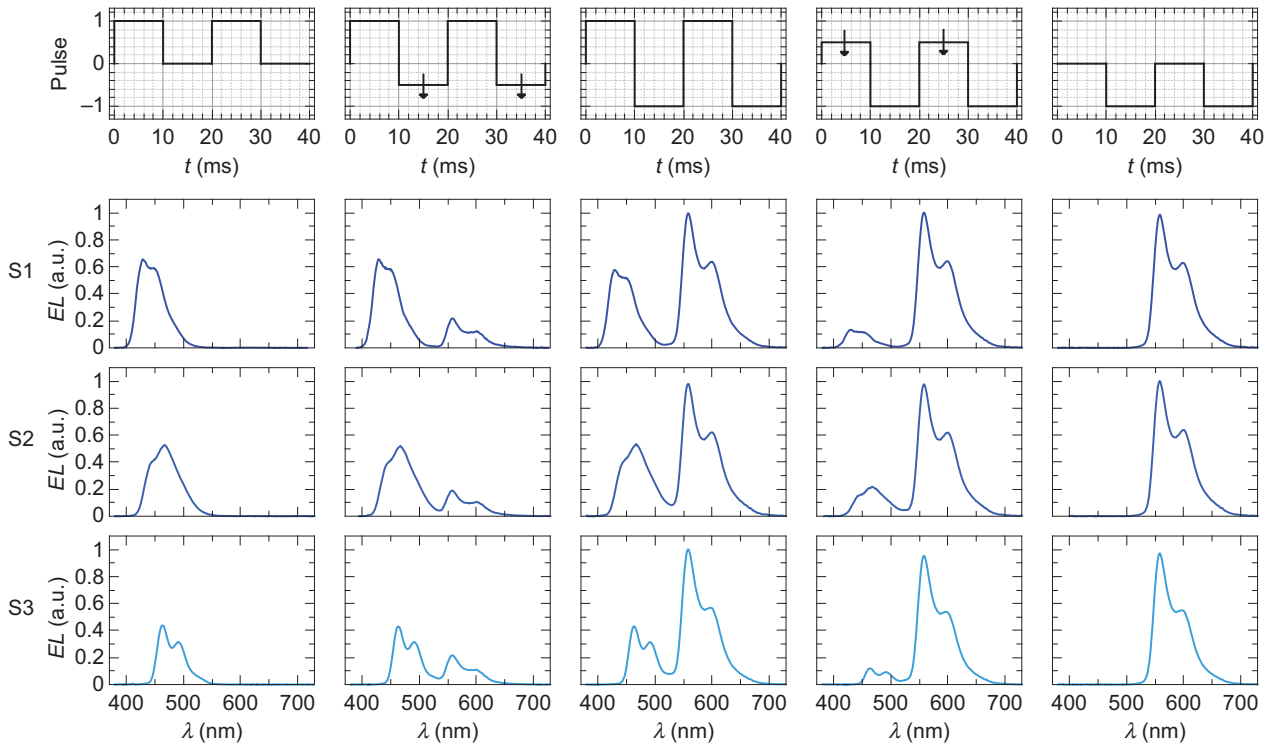

Figure 3 Emission spectra of S1, S2 and S3 when the five different 50 Hz square-wave signals depicted in the top row are applied. Columns 1 and 5 represent pure emission from the blue or yellow unit, as either the negative or the positive half-cycle is zero. Column 3 represents mixed emission from both units when the samples are driven by a symmetrical signal. Intermediate waveforms lead to a reduced contribution from one of the emission units (columns 2 and 4).

voltage pulse intensities and hence the fractions of blue and yellow emission contributing to the resulting spectrum. The color-tuning curves of S1 (4P-NPD) and S2 (PPIP) intersect the Planckian locus (i.e., the line that describes radiation from black-body radiators at various temperatures); for S1, this intersection is very close to the warm-white color reference point A.

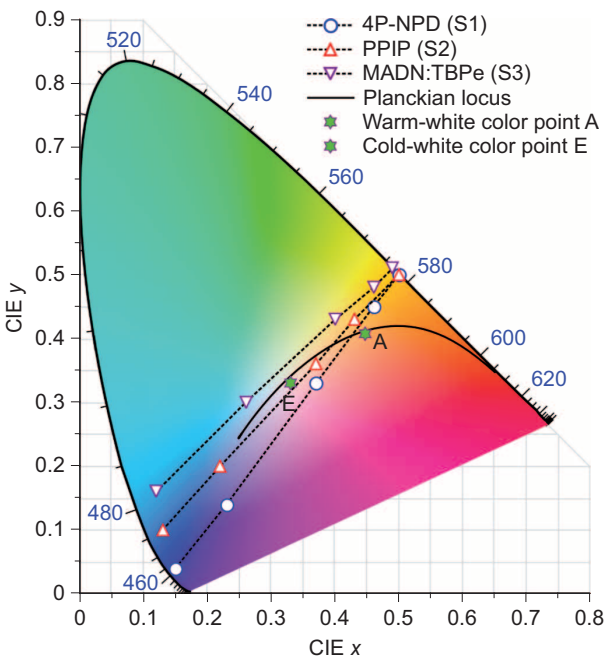

Figure 4 Color coordinates corresponding to the emission spectra presented in Figure 3 for S1, S2 and S3.

As the next step, we measured the *LE*s of S1, S2 and S3 at a brightness of 1000 cd m^{-2} when the devices were tuned to warm-white color coordinates. For this experiment, color tuning was performed by adjusting the 'on time' of each unit, i.e., by varying the relative pulse widths of the positive and negative half-cycles at equal and constant pulse heights or driving voltages. Compared with the previously demonstrated pulse height modulation, this approach allows for finer tuning of the emission color, as small changes in the on time ratio between the two units also lead to small shifts in emission color. By contrast, small variations in the driving voltage result in large variations in luminance (because of the super-linear diode behavior of the individual units) which lead to strong color shifts. For all three samples, Table 1 summarizes the *LE*, the CIE color coordinates, the color rendering index (CRI) and the on time ratio between the blue and yellow units that was required to reach the color point A. Samples S2 (PPIP) and S3 (MADN:TBPe) achieved *LE*s of 31.5 lm W^{-1} and 27.9 lm W^{-1}, respectively.

Interestingly, the white AC/DC OLED with 4P-NPD achieved the highest *LE*, although the *LE* of 4P-NPD is considerably lower than those of the other two blue emitters (cf. Figure 2d). This observation is explained by the considerable difference in *LE* between the blue and yellow emitter systems (cf. Figure 2c and 2d), as the phosphorescent yellow unit has a 40-fold higher *LE* than does the fluorescent blue unit. It is therefore important to maximize the on time of the yellow emitter and keep the contribution of the blue emitter to a minimum. Considering the on time ratios of the three emitter systems under investigation (cf. Table 1), we find that this is best achieved using

doi:10.1038/lsa.2015.20

Table 1 CIE color coordinates, CRI, on time ratio of the blue and yellow units, and luminous efficacy for S1, S2 and S3

Sample	Blue emitter	CIE	CRI	On time (%)[a] blue unit/yellow unit	Luminous efficacy[b] (lm W^{-1})
S1	4P-NPD	(0.44,0.45)	38	15/85	36.8
S2	PPIP	(0.44,0.47)	36	20/80	31.5
S3	MADN : TBPe	(0.41,0.44)	35	30/70	27.9

Abbreviation: CRI, color rendering index.
[a] 50 Hz AC signal, 2.93 V_{rms}, equal pulse heights for positive and negative half-cycles.
[b] At a brightness of 1000 cd m^{-2}.

the deep-blue emitter 4P-NPD, for which the on time of the blue unit for warm-white emission is merely 15%. The more sky-blue emitters PPIP and MADN:TBPe require increased on times of 20% and 30%, respectively, resulting in reduced *LE*s compared with the 4P-NPD sample. The obtained efficiency value of 36.8 lm W^{-1} is even higher than the value of 32.6 lm W^{-1} that has recently been achieved for non-color-tunable white OLEDs using the same emitter materials in a triplet-harvesting configuration[27] and, to our knowledge, represents the best efficiency achieved thus far for any freely color-tunable white OLED. As previously mentioned, the high efficiency of AC/DC OLEDs results predominantly from the high efficiency of the yellow unit, which can operate close to its maximum internal quantum efficiency because of the direct electrical excitation. By contrast, the internal quantum efficiency of the yellow emitter in the triplet-harvesting white OLED is limited to approximately 50% because of the moderate exciton-harvesting efficiency.[27]

The low CRI values for all three samples (cf. Table 1) result from the combination of only two emitters (blue and yellow) to obtain white light, which means that important contributions in the green and deep-red spectral regions are missing. However, as the device design of AC/DC OLEDs is highly flexible in terms of emitter combinations, this problem of low CRI can be addressed quite easily, e.g., by modifying the blue emission unit into a blue+red triplet-harvesting emission unit and replacing the yellow phosphor with a green phosphorescent emitter. The presence of red, green and blue emitters would guarantee a high CRI, and the combination of a highly efficient triplet-harvesting unit (blue+red can be more efficient than blue+yellow because of the more favorable relative triplet energy levels) and a phosphorescent green emitter is expected to result in high overall efficiency.

The operational stability of AC/DC white OLEDs is comparable to that of conventional DC-driven white OLEDs, and in preliminary tests, we did not observe any adverse effects of driving these devices with an AC signal instead of the commonly used DC bias.

CONCLUSIONS

In summary, we demonstrated highly efficient color-tunable AC/DC OLEDs based on a combination of a blue-emitting unit and a yellow-emitting unit. The fabrication and electrical driving of these devices were simplified by reducing the number of independent electrodes to two and using an AC voltage for color tuning. Color tuning can be accomplished either by modifying the pulse height or by adjusting the pulse width ratio between the positive and negative half-cycles of the AC signal. The influence of the central electrode on the optical characteristics of the OLEDs was reduced by using a highly transparent thin-film metal electrode. In combination with the deep-blue fluorescent emitter 4P-NPD, this leads to an impressive luminous efficacy of 36.8 lm W^{-1} at warm-white color coordinates of (0.44,0.45) and at brightness levels compatible with application requirements (1000 cd m^{-2}). All efficacy values reported here were obtained without any outcoupling enhancement. By integrating well-established light-extraction techniques, a two- to three-fold improvement in luminous efficacy can be achieved.[28]

To demonstrate the versatility of our approach and to investigate the influence of different blue emitters on the device performance, measurements were performed using the sky-blue emitter systems PPIP and MADN:TBPe. These measurements indicated that the use of a deep-blue emitter such as 4P-NPD is beneficial for obtaining a high luminous efficacy, as it allows the on time of the blue unit to be reduced.

In future work, this concept could be extended to three pin-OLEDs stacked on top of each other to provide red, green, and blue emission. This configuration is particularly interesting for display applications, in which a vertical stacking of the red, green and blue sub-pixels would allow for higher pixel densities and an optimal fill factor in comparison with conventional side-by-side fabrication.

ACKNOWLEDGEMENTS

This work was funded by the European Social Fund and the Free State of Saxony through the OrthoPhoto project. We kindly acknowledge the support from NUDEV.

1 Sasabe H, Kido J. Development of high performance OLEDs for general lighting. *J Mater Chem C* 2013; **1**: 1699–1707.
2 Reineke S, Lindner F, Schwartz G, Seidler N, Walzer K *et al*. White organic light-emitting diodes with fluorescent tube efficiency. *Nature* 2009; **459**: 234–238.
3 Rosenow TC, Furno M, Reineke S, Olthof S, Lüssem B *et al*. Highly efficient white organic light-emitting diodes based on fluorescent blue emitters. *J Appl Phys* 2010; **108**: 113113.
4 OLED-Info.com. *Beautiful OLED lighting designs at LG's design contest*. Available at http://www.oled-info.com/beautiful-oled-lighting-designs-lgs-design-contest (accessed August 2014).
5 Berggren M, Inganäs O, Gustafsson G, Rasmusson J, Andersson MR *et al*. Light-emitting diodes with variable colours from polymer blends. *Nature* 1994; **372**: 444–446.
6 Yang Y, Pei Q. Voltage controlled two color light-emitting electrochemical cells. *Appl Phys Lett* 1996; **68**: 2708.
7 Gather MC, Alle R, Becker H, Meerholz K. On the origin of the color shift in white-emitting OLEDs. *Adv Mater* 2007; **19**: 4460–4465.
8 Burrows PE, Forrest SR, Sibley SP, Thompson ME. Color-tunable organic light-emitting devices. *Appl Phys Lett* 1996; **69**: 2959.
9 Parthasarathy G, Gu G, Forrest SR. A full-color transparent metal-free stacked organic light emitting device with simplified pixel biasing. *Adv Mater* 1999; **11**: 907–910.
10 Shen Z, Burrows PE, Bulovic V, Forrest SR, Thompson ME. Three-color, tunable, organic light-emitting devices. *Science* 1997; **276**: 2009–2011.
11 Kim HK, Kim DG, Lee KS, Huh MS, Jeong SH *et al*. Plasma damage-free sputtering of indium tin oxide cathode layers for top-emitting organic light-emitting diodes. *Appl Phys Lett* 2005; **86**: 183503.
12 Deppe DG, Lei C, Lin CC, Huffaker DL. Spontaneous emission from planar microstructures. *J Mod Opt* 1994; **41**: 325–344.
13 Becker H, Burns SE, Tessler N, Friend RH. Role of optical properties of metallic mirrors in microcavity structures. *J Appl Phys* 1997; **81**: 2825.
14 Zhang XW, Li J, Zhang L, Jiang XY, Haq K *et al*. Top-emitting organic light-emitting device with high efficiency and low voltage using a silver–silver microcavity. *Thin Solid Films* 2010; **518**: 1756–1759.
15 Jiang Y, Lian J, Chen S, Kwok HS. Fabrication of color tunable light-emitting diodes by an alignment free mask patterning method. *Org Electr* 2013; **14**: 2001–2006.

16 Joo CW, Moon J, Han JH, Huh JW, Lee J *et al*. Color temperature tunable white light-emitting diodes. *Org Electr* 2014; **15**: 189–195.
17 Gu G, Khalfin V, Forrest SR. High-efficiency, low-drive-voltage, semitransparent stacked organic light-emitting device. *Appl Phys Lett* 1998; **73**: 2399.
18 Liang CJ, Choy WCH. Tunable full-color emission of two-unit stacked organic light-emitting diodes with dual-metal intermediate electrode. *J Organomet Chem* 2009; **694**: 2712–2716.
19 Schubert S, Meiss J, Müller-Meskamp L, Leo K. Improvement of transparent metal top electrodes for organic solar cells by introducing a high surface energy seed layer. *Adv Energy Mater* 2013; **3**: 438–443.
20 Schwab T, Schubert S, Hofmann S, Fröbel M, Fuchs C *et al*. Highly efficient color stable inverted white top-emitting OLEDs with ultra-thin wetting layer top electrodes. *Adv Opt Mater* 2013; **1**: 707–713.
21 Schwab T, Schubert S, Müller-Meskamp L, Leo K, Gather MC. Eliminating microcavity effects in white top-emitting OLEDs by ultra-thin metallic top electrodes. *Adv Opt Mater* 2013; **1**: 921–925.
22 Perumal A, Fröbel M, Gorantla S, Gemming T, Lüssem B *et al*. Novel approach for alternating current (AC)-driven organic light-emitting devices. *Adv Funct Mater* 2012; **22**: 210–217.
23 Fröbel M, Perumal A, Schwab T, Gather MC, Lüssem B *et al*. Enhancing the efficiency of alternating current driven organic light-emitting devices by optimizing the operation frequency. *Org Electr* 2013; **14**: 809–813.
24 Fröbel M, Perumal A, Schwab T, Fuchs C, Leo K *et al*. White light emission from alternating current organic light-emitting devices using high frequency color-mixing. *Phys Status Solidi A* 2013; **210**: 2439–2444.
25 Huang J, Pfeiffer M, Werner A, Blochwitz J, Leo K *et al*. Low-voltage organic electroluminescent devices using pin structures. *Appl Phys Lett* 2002; **80**: 139.
26 Kuo CJ, Li TY, Lien CC, Liu CH, Wu FI *et al*. Bis(phenanthroimidazolyl)biphenyl derivatives as saturated blue emitters for electroluminescent devices. *J Mater Chem* 2009; **19**: 1865–1871.
27 Hofmann S, Furno M, Lüssem B, Leo K, Gather MC. Investigation of triplet harvesting and outcoupling efficiency in highly efficient two-color hybrid white organic light-emitting diodes. *Phys Status Solidi A* 2013; **210**: 1467–1475.
28 Saxena K, Jain V, Mehta DS. A review on the light extraction techniques in organic electroluminescent devices. *Opt Mater* 2009; **32**: 221–233.

Supplementary information for this article can be found on the *Light: Science & Applications*' website (http://www.nature.com/lsa/).